PROCEEDINGS of the
23rd International Congress on Acoustics

9 to 13 September 2019 in Aachen, Germany

Prediction of the sound transmission loss of two-dimensional periodic structures with a hybrid framework

Carolina DECRAENE(1), Edwin P.B. REYNDERS(2), Geert LOMBAERT(3)

(1)Structural Mechanics Section, Dept. of Civil Engineering, KU Leuven, Belgium, carolina.decraene@kuleuven.be

(2)Structural Mechanics Section, Dept. of Civil Engineering, KU Leuven, Belgium, edwin.reynders@kuleuven.be

(3)Structural Mechanics Section, Dept. of Civil Engineering, KU Leuven, Belgium, geert.lombaert@kuleuven.be

Abstract

The diffuse sound transmission through a complex finite-sized wall or floor can be efficiently computed with a hybrid approach. The wall is then modelled deterministically as finite size effects and modal behaviour can be important in this frequency range, while the rooms carry a diffuse field and are modelled as stochastic subsystems. The finite element method is usually employed to compute the modal behaviour of the wall. At higher frequencies, the computational cost then increases significantly as a finer mesh is required due to the shorter wavelength of structural deformation. For this reason, an alternative approach was recently developed, which allows to replace the finite element model by an analytical model for finite-sized thick and layered walls. However, the application of this approach is limited to layered structures such as sandwich panels or double glazing. In the present work, the elaboration towards more complicated building elements which exhibit spatial periodicity, will be considered by invoking periodic structure theory. As a first validation example, a steel panel is considered, in which the predictions are compared to other numerical and experimental data.

Keywords: sound transmission loss, periodic, hybrid

1 INTRODUCTION

Lightweight systems are more frequently used in buildings to achieve a high thermal performance and to save material and transportation costs. Because of their relatively low weight and complex vibro-acoustic behaviour, achieving a sufficient level of sound insulation with such systems is, however, challenging. The goal in this work is to create an accurate sound transmission loss prediction method, which is efficient enough to be used as a design tool and can replace the need of excessive experimental prototype testing.

The framework of the hybrid finite element-statistical energy analysis (FE-SEA) approach [1, 2, 3] serves as a starting point in this article. Using the diffuse field reciprocity relationship [4, 5], the hybrid framework allows modelling the rooms of the overall room-wall-room system as stochastic subsystems (like in statistical energy analysis, SEA), while treating the wall in a deterministic way with finite element (FE) analysis. A diffuse field model is by definition a stochastic model. The uncertainty of the sound transmission loss concerning the diffuse field assumption in the SEA subsystems can be assessed [3]. This allows computing the mean of the sound transmission loss as well as its variance. Note that the computation time of the FE-SEA method will increase at higher frequencies as a finer mesh is needed to capture the small wavelength deformations of the structure.

To overcome this limitation, two alternative approaches were already explored. First, the finite element analysis could be replaced with a semi-analytical transfer matrix method (TMM) [6, 7, 8], which allows to predict the behaviour of infinite walls and floors, consisting of homogeneous solid, fluid and/or poroelastic layers. By projecting the wall displacements onto a set of sinusoidal lateral basis functions [9, 10], the modal behaviour of the structure is approximately taken into account. This recently developed approximate modal TMM-SEA approach (mTMM-SEA) is however limited to layered systems [11].

Secondly, a hybridization between periodic finite element modelling (peFE) and statistical energy analysis was achieved in [12]. The periodic lay out of most building elements could therefore be exploited. The latter peFE-SEA approach has two challenges that must be tackled: (1) modal behaviour, which influences the sound

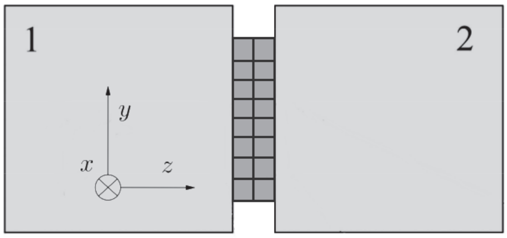

Figure 1. A room-wall-room system, in which the wall is modelled in a deterministic way while the rooms are modelled as SEA subsystems.

transmission loss in the considered frequency range (50-3150 Hz), is disregarded; (2) computing the sound transmission loss results in an integration over each phase constant surface in the phase lag domain and is thus computationally inefficient. The two problems are solved by discretizing the phase domain into the phase combinations causing standing waves in the structure. Ideas in this direction were already mentioned in [12]. Whereas the authors in [12] focus mainly on Born-von Kármán boundary conditions, the wall or floor in the present work is assumed to have simply supported boundary conditions, because modal testing has revealed that simply supported boundary conditions occur in the small transmission opening of the KU Leuven Laboratory of Acoustics [13]. Contributions of the present work include also a theoretical expansion of the method with special attention to implementation issues and a detailed validation example.

The remainder of this article is organized as follows. The theory is summarized in section 2. Section 2.1 introduces the hybrid deterministic-SEA approach to sound transmission modelling in general. Section 2.2 elaborates periodic structure theory with emphasis on obtaining the necessary dynamic stiffness matrices. In section 3 the method is validated for a steel plate by comparing the predicted sound transmission loss with other prediction tools and with experimental data. The conclusions are to be found in section 4.

2 A HYBRID MODAL BASED PERIODIC FINITE ELEMENT-SEA APPROACH

2.1 The hybrid framework

Throughout this article, a room-wall-room system is considered, where the rooms carry a diffuse wave field and the wall a deterministic wave field (cfr. Fig. 1). The out-of-plane displacement u_z of the partition wall at position $\mathbf{x} = (x, y)$ and at frequency ω is decomposed using a finite set of N_{dof} global basis functions $\hat{\boldsymbol{\varphi}}$ and corresponding generalized coordinates $\mathbf{a}$:

$$u_z(\mathbf{x}, \omega) \approx \sum_{p=1}^{N_{\text{dof}}} \hat{\boldsymbol{\varphi}}_p(\mathbf{x}) a_p(\omega) \tag{1}$$

All generalized response degrees of freedom (DOFs) are collected in the vector $\mathbf{a}(\omega) \in \mathbb{C}^{N_{\text{dof}}}$, so that the time-domain response is given by $\text{Re}(\mathbf{a}e^{i\omega t})$, with i the imaginary unit. Similarly, the corresponding generalized harmonic loads are collected in the load amplitude vector $\mathbf{f}(\omega) \in \mathbb{C}^{N_{\text{dof}}}$. Since $\mathbf{a}$ contains all (generalized) interface degrees of freedom between the wall and the rooms, the equations of motion of the whole system (room-wall-room) can be written as

$$\mathbf{D}\mathbf{a} = \mathbf{f}, \tag{2}$$

with $\mathbf{D} \in \mathbb{C}^{N_{\text{dof}} \times N_{\text{dof}}}$ the dynamic stiffness matrix at frequency ω. $\mathbf{D}$ may be decomposed into the dynamic stiffness matrix of the wall, denoted as $\mathbf{D}_{\text{d}}$ (subscript d stands for deterministic), and the dynamic stiffness matrices of the rooms, denoted as $\mathbf{D}_1$ and $\mathbf{D}_2$:

$$\mathbf{D} = \mathbf{D}_{\mathrm{d}} + \mathbf{D}_1 + \mathbf{D}_2 \tag{3}$$

Since the rooms are assumed to carry a diffuse field in this work, they are modelled as random subsystems in the overall room-wall-room system. The dynamic stiffness matrix of each acoustic room volume k is decomposed as

$$\mathbf{D}_k = \mathbf{D}_{\mathrm{dir}}^{(k)} + \mathbf{D}_{\mathrm{rev}}^{(k)}, \qquad k = 1,2 \tag{4}$$

where $\mathbf{D}_{\mathrm{dir}}^{(k)}$ denotes the mean of the subsystem's dynamic stiffness matrix $\mathbf{D}_{\mathrm{dir}}^{(k)} := \mathrm{E}\left[\mathbf{D}_k\right]$. This term describes the response of subsystem k to the outgoing wave field caused by the displacements of the deterministic boundary [4, 14]. Boundaries and objects in the room induce however random wave scattering. The influence of this reverberant field on subsystem k is captured by $\mathbf{D}_{\mathrm{rev}}^{(k)}$. With this decomposition, the equations of motion for a random subsystem are

$$\mathbf{D}_{\mathrm{dir}}^{(k)}\mathbf{a} = -\mathbf{f}_k - \mathbf{f}_{\mathrm{rev}}^{(k)}, \tag{5}$$

where the reverberant forces are defined as $\mathbf{f}_{\mathrm{rev}}^{(k)} := -\mathbf{D}_{\mathrm{rev}}^{(k)}\mathbf{a}$, and $\mathbf{f}_k$ denotes the sum of the loads applied to subsystem k at its DOFs. The overall equations of motion (2) become

$$\mathbf{D}_{\mathrm{tot}}\mathbf{q} = \mathbf{f} - \mathbf{f}_{\mathrm{rev}}^{(1)} - \mathbf{f}_{\mathrm{rev}}^{(2)}, \tag{6}$$

where $\mathbf{D}_{\mathrm{tot}} := \mathbf{D}_{\mathrm{d}} + \sum_{k=1}^{2} \mathbf{D}_{\mathrm{dir}}^{(k)}$ is a purely deterministic matrix. When a diffuse field acts in both rooms, the reverberant forces $\mathbf{f}_{\mathrm{rev}}^{(k)}$ are related to $\mathbf{D}_{\mathrm{dir}}^{(k)}$ through the diffuse field reciprocity relationship [4]:

$$\mathrm{E}[\mathbf{f}_{\mathrm{rev}}^{(k)}\mathbf{f}_{\mathrm{rev}}^{(s)}] = \delta_{ks}\frac{4\hat{E}_k}{\omega\pi n_k}\mathrm{Im}\left(\mathbf{D}_{\mathrm{dir}}^{(k)}\right), \tag{7}$$

with n_k the modal density of subsystem k [15] and δ_{ks} the Kronecker delta. Note that the hat symbol is employed here as shorthand notation for ensemble mean. Using this equation, it is possible to obtain the mean time-averaged total energy $\hat{E}_k$ of room k from a stationary power balance which involves the other random subsystems as well as the deterministic master system, assuming the fields are statistically independent of each other. For the case where the external loading acts solely on the random subsystems (rooms), the power balance is formulated as [1]:

$$\omega\left(\eta_k + \hat{\eta}_{\mathrm{d},k}\right)\hat{E}_k + \sum_{j=1}^{2}\omega\hat{\eta}_{kj}n_k\left(\frac{\hat{E}_k}{n_k} - \frac{\hat{E}_j}{n_j}\right) = \hat{P}_k, \qquad k = 1,2. \tag{8}$$

In this expression, η_k is the damping loss factor of subsystem k, P_k the power input from external loading injected directly into the diffuse field of this subsystem, and

$$\hat{\eta}_{\mathrm{d},k} = \frac{2}{\omega\pi n_k}\sum_{r,s}\mathrm{Im}\left(D_{\mathrm{d},rs}\right)\left(\mathbf{D}_{\mathrm{tot}}^{-1}\mathrm{Im}\left(\mathbf{D}_{\mathrm{dir}}^{(k)}\right)\mathbf{D}_{\mathrm{tot}}^{-\mathrm{H}}\right)_{rs} \tag{9}$$

$$\hat{\eta}_{kj} = \frac{2}{\omega\pi n_k}\sum_{r,s}\mathrm{Im}\left(D_{\mathrm{dir},rs}^{(k)}\right)\left(\mathbf{D}_{\mathrm{tot}}^{-1}\mathrm{Im}\left(\mathbf{D}_{\mathrm{dir}}^{(j)}\right)\mathbf{D}_{\mathrm{tot}}^{-\mathrm{H}}\right)_{rs} \tag{10}$$

where the superscript H denotes Hermitian transpose and the integer subscripts r,s select an element in row r and column s of a matrix. When the sound insulation provided by the wall is sufficiently high, $\hat{P}_k$ can be approximated as the ensemble mean of the power input into a hard-walled room. It can be noted that the power balance equation (8) has formally the same structure as in conventional SEA. Therefore the factors $\hat{\eta}_{kj}$ can be interpreted as coupling loss factors, and (10) provides a rigorous way to compute their ensemble mean. In a similar manner, (9) enables to rigorously estimate the power that is lost by energy dissipation in the wall. By solving for the mean coupling loss factor $\hat{\eta}_{12}$ between the two subsystems, the mean sound transmission coefficient $\hat{\tau}_{12}$ can be obtained from [15]

$$\hat{\tau}_{12} = \hat{\eta}_{12} \frac{4\omega V_1}{c_a S}, \tag{11}$$

with S the surface area of the wall, V_1 the volume of the sending room, and c_a the speed of sound. Note that the dynamic stiffness matrices are diagonal when cross modal coupling is neglected, in which case equation (11) can be rewritten as:

$$\hat{\tau}_{12} = \frac{16\pi}{S k_a^2} \left[\sum_p \frac{\mathrm{Im}\{D^{(2)}_{\mathrm{dir},p}\} \mathrm{Im}\{D^{(1)}_{\mathrm{dir},p}\}}{|D_{\mathrm{tot},p}|^2} \right] \tag{12}$$

where k_a is the acoustic wavenumber.

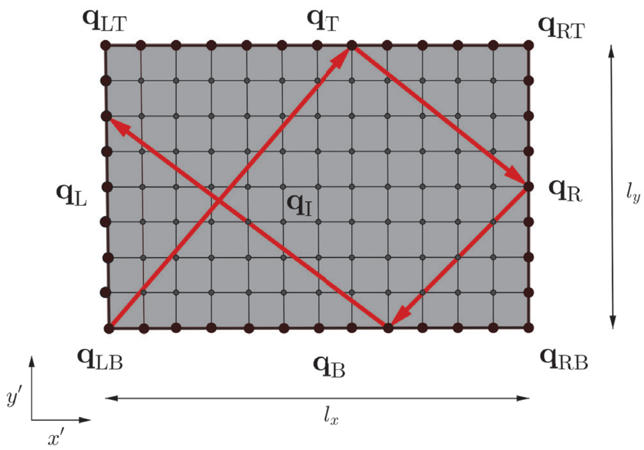

Figure 2. Indication of the edge and corner degrees of freedom of a periodic unit cell. The red arrows show the path of a travelling wave, reflected at the edges. Combination of these four waves result in a standing wave.

2.2 Determining $\mathbf{D}_{\mathrm{d}}$ and $\mathbf{D}_{\mathrm{dir}}$ using periodic structure theory

If a two-dimensional periodic structure with dimensions $L_x \times L_y$ is considered, it is possible to extract a periodic unit cell which is repeated N_x and N_y times within the structure in respectively the x- and y-direction. A finite element model of such a unit cell with dimensions l_x and l_y is shown in figure 2 where the local coordinate system is denoted by $\mathbf{x}' = (x', y')$. The degrees of freedom $\mathbf{q}$ of the unit cell are reorganized into interior (I=interior), edge (T=Top, B=Bottom, R=Right, L=Left) and corner DOFs (LB, RB, LT, RT). The dynamic response of the unit cell is then investigated using Bloch's theorem, in which periodic boundary conditions are imposed onto the edge and corner DOFs [16, 17, 18, 19, 20]. Defining the phase lag combination $(\varepsilon_{xp}, \varepsilon_{yq})$, the relations between the boundary DOFs can be written in matrix format:

$$\mathbf{q} = \begin{bmatrix} \mathbf{q}_\mathrm{I} \\ \mathbf{q}_\mathrm{B} \\ \mathbf{q}_\mathrm{T} \\ \mathbf{q}_\mathrm{L} \\ \mathbf{q}_\mathrm{R} \\ \mathbf{q}_\mathrm{LB} \\ \mathbf{q}_\mathrm{RB} \\ \mathbf{q}_\mathrm{LT} \\ \mathbf{q}_\mathrm{RT} \end{bmatrix} = \begin{bmatrix} \mathbf{I} & \mathbf{0} & \mathbf{0} & \mathbf{0} \\ \mathbf{0} & \mathbf{I} & \mathbf{0} & \mathbf{0} \\ \mathbf{0} & \mathbf{I}\mathrm{e}^{-\mathrm{i}\varepsilon_{yq}} & \mathbf{0} & \mathbf{0} \\ \mathbf{0} & \mathbf{0} & \mathbf{I} & \mathbf{0} \\ \mathbf{0} & \mathbf{0} & \mathbf{I}\mathrm{e}^{-\mathrm{i}\varepsilon_{xp}} & \mathbf{0} \\ \mathbf{0} & \mathbf{0} & \mathbf{0} & \mathbf{I} \\ \mathbf{0} & \mathbf{0} & \mathbf{0} & \mathbf{I}\mathrm{e}^{-\mathrm{i}\varepsilon_{xp}} \\ \mathbf{0} & \mathbf{0} & \mathbf{0} & \mathbf{I}\mathrm{e}^{-\mathrm{i}\varepsilon_{yq}} \\ \mathbf{0} & \mathbf{0} & \mathbf{0} & \mathbf{I}\mathrm{e}^{-\mathrm{i}\varepsilon_{xp}-\mathrm{i}\varepsilon_{yq}} \end{bmatrix} \begin{bmatrix} \mathbf{q}_\mathrm{I} \\ \mathbf{q}_\mathrm{B} \\ \mathbf{q}_\mathrm{L} \\ \mathbf{q}_\mathrm{LB} \end{bmatrix} = \mathbf{R}\mathbf{q}' \tag{13}$$

with $\mathbf{q}' = [\mathbf{q}_\mathrm{I}^\mathrm{T}\ \mathbf{q}_\mathrm{B}^\mathrm{T}\ \mathbf{q}_\mathrm{L}^\mathrm{T}\ \mathbf{q}_\mathrm{LB}^\mathrm{T}]^\mathrm{T}$ the reduced DOFs. This reduction is then applied to the equations of motion of the unit cell as well, so that the following reduced eigenvalue problem is obtained:

$$[\mathbf{K}' - \omega^2\mathbf{M}']\mathbf{q}' = \mathbf{0} \tag{14}$$

where $\mathbf{K}' = \mathbf{R}^\mathrm{H}(\varepsilon_{xp}, \varepsilon_{yq})\mathbf{K}\mathbf{R}(\varepsilon_{xp}, \varepsilon_{yq})$ and $\mathbf{M}' = \mathbf{R}^\mathrm{H}(\varepsilon_{xp}, \varepsilon_{yq})\mathbf{M}\mathbf{R}(\varepsilon_{xp}, \varepsilon_{yq})$ are respectively the reduced mass and stiffness matrix of the periodic unit cell. As modal behaviour is investigated, only phase constants that allow standing waves in the structure need to be considered. For a mode of the system, the summation of the phase constants of a back and forward travelling wave in the global structure adds up to a multiplication of 2π, so that [22]:

$$\varepsilon_{xp} = p\pi/N_x \qquad (p = 0, \ldots, N_x) \qquad \text{and} \qquad \varepsilon_{yq} = q\pi/N_y, \qquad (q = 0, \ldots, N_y)$$

For each phase constant combination $(\varepsilon_{xp}, \varepsilon_{yq})$, the eigenvalue problem in equation (14) is solved for a number of possible corresponding eigenfrequencies $\Omega_{pq,n}$ and corresponding eigenvectors $\boldsymbol{\varphi}_{pq,n}(\mathbf{x}')$ as multiple waves can propagate under an imposed periodic boundary condition. Note that the mode shapes of the unit cell are mass normalized: $\boldsymbol{\varphi}_{pq,n}^\mathrm{H}\mathbf{M}'\boldsymbol{\varphi}_{pq,n} = 1$. Post-processing the results includes (1) selecting only the normal displacements; (2) converting standing waves into travelling waves at the edges and corners of the phase domain. This is necessary to guarantee the correct use of the proposed general method, which accounts for a two-dimensional travelling wave; (3) eliminating waves with zero wavenumber in x- or y- direction as they do not add up to a standing wave in one direction and (4) eliminating the phase shift of the travelling waves to ensure zero displacements at the boundary of the global structure. The obtained dynamic properties of the unit cell are now used to determine the direct field response of the subsystems and the deterministic response of the wall, which in their turn will be inserted into the hybrid framework.

First, the direct field dynamic stiffness matrix $D_{\mathrm{dir},pq,n}$ of standing wave pq,n is determined as follows:

$$D_{\mathrm{dir},pq,n}(\omega) = \frac{1}{4\pi^2}\int_{-\infty}^{\infty}\int_{-\infty}^{\infty} G^*(\omega, \mathbf{k}, z = 0)|\boldsymbol{\psi}_{pq,n}(\mathbf{k})|^2 \mathrm{d}\mathbf{k}, \tag{15}$$

in which $G(\omega, \mathbf{k}, z = 0) = \frac{\mathrm{i}\omega^2\rho_a}{\sqrt{k_a^2 - ||\mathbf{k}^2||}}$ is the Green's function with ρ_a the density of air. To avoid singularity at coincidence, a Green's function averaged in the wavenumber domain was used [21]. Assuming simply supported boundary conditions, the displacement field $\boldsymbol{\psi}_{pq,n}(\mathbf{x})$ consists of four travelling waves with the same eigenfrequency as illustrated in figure 2: $\hat{\boldsymbol{\varphi}}_{pq,n}(\mathbf{x})$, $\hat{\boldsymbol{\varphi}}_{(-p)q,n}(\mathbf{x})$, $\hat{\boldsymbol{\varphi}}_{p(-q),n}(\mathbf{x})$ and $\hat{\boldsymbol{\varphi}}_{(-p)(-q),n}(\mathbf{x})$. Because $\hat{\boldsymbol{\varphi}}_{(-p)(-q),n} = \hat{\boldsymbol{\varphi}}^*_{pq,n}$ and $\hat{\boldsymbol{\varphi}}_{(-p)q,n} = \hat{\boldsymbol{\varphi}}^*_{p(-q),n}$ with $*$ indicating the complex conjugate, the standing wave in the wavenumber domain $\mathbf{k} = (k_x, k_y)$ is found by:

$$\boldsymbol{\psi}_{pq,n}(\mathbf{k}) = \hat{\boldsymbol{\varphi}}_{pq,n}(\mathbf{k}) + \hat{\boldsymbol{\varphi}}^*_{pq,n}(-\mathbf{k}) - \hat{\boldsymbol{\varphi}}_{p(-q),n}(\mathbf{k}) - \hat{\boldsymbol{\varphi}}^*_{p(-q),n}(-\mathbf{k}) \tag{16}$$

The travelling wave of the total structure $\hat{\boldsymbol{\varphi}}_{pq,n}(\mathbf{k})$ is derived from the obtained eigenvectors of the unit cell $\boldsymbol{\varphi}_{pq,n}(\mathbf{k})$ using the following relation [12]:

$$\hat{\boldsymbol{\varphi}}_{pq,n}(\mathbf{k}) = \boldsymbol{\varphi}_{pq,n}(\mathbf{k})\left(\frac{1 - \mathrm{e}^{-\mathrm{i}N_x(\varepsilon_x - k_x l_x)}}{1 - \mathrm{e}^{-\mathrm{i}(\varepsilon_x - k_x l_x)}}\right) \cdot \left(\frac{1 - \mathrm{e}^{-\mathrm{i}N_y(\varepsilon_y - k_y l_y)}}{1 - \mathrm{e}^{-\mathrm{i}(\varepsilon_y - k_y l_y)}}\right) \tag{17}$$

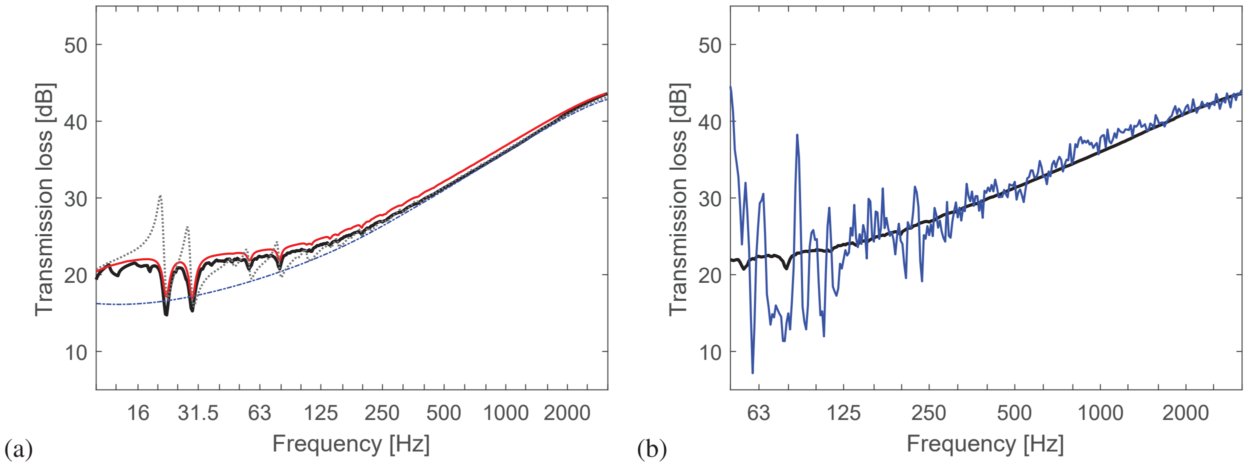

Figure 3. Harmonic sound transmission loss of a steel plate (a) as predicted with the hybrid modal peFE-SEA approach (black continuous line), the FTMM (blue dashed line), the hybrid mTMM-SEA method for which cross modal coupling is neglected (red line), the hybrid mTMM-SEA with cross modal coupling (black dotted line); and (b) as measured in the Acoustic Laboratory of the KU Leuven (blue continuous line).

$\boldsymbol{\varphi}_{pq,n}(\mathbf{k})$ and $\boldsymbol{\varphi}_{p(-q),n}(\mathbf{k})$ follow from a Fourier transform of $\boldsymbol{\varphi}_{pq,n}(\mathbf{x}')$ and $\boldsymbol{\varphi}_{p(-q),n}(\mathbf{x}')$. As $\boldsymbol{\varphi}_{p(-q),n}(\mathbf{x}')$ can be computed from $\boldsymbol{\varphi}_{pq,n}(\mathbf{x}')$ by mirroring the displacement field around the x-axis, the eigenvalue problem for the phase constant combination (p,q) only needs to be performed once. Note that the mesh in the $\mathbf{x}$-domain needs to be more refined for the computation of the direct field response than required for the FE analysis of the periodic unit cell. Decoupling this so-called acoustic mesh and the FE mesh is therefore recommended.

Secondly, the deterministic dynamic stiffness matrix $D_{\mathrm{d},pq,n}$ is determined by:

$$D_{\mathrm{d},pq,n} = 4N_xN_y\left((1+\mathrm{i}\eta)\Omega_{pq,n}^2 - \omega^2\right) \tag{18}$$

with η the loss factor of the structure.

3 VALIDATION EXAMPLE: STEEL PLATE

The modal peFE-SEA is applied to a thin, simply supported steel plate. The steel plate has a density $\rho = 7750\,\frac{\mathrm{kg}}{\mathrm{m}^3}$, Young's modulus $E = 200\,\mathrm{GPa}$, Poisson's ratio $\nu = 0.28$ and dimensions $1.25\,\mathrm{m} \times 1.50\,\mathrm{m} \times 0.002\,\mathrm{m}$. The experimentally determined damping loss factor of the mounted plate can be found in [11]. In the simulations, the reverberation time T, the air density ρ_a and the sound speed c_a in the rooms are taken to be $1.5\,\mathrm{s}$, $1.2\,\frac{\mathrm{kg}}{\mathrm{m}^3}$ and $343\,\frac{\mathrm{m}}{\mathrm{s}}$, respectively. Specifically for the considered peFE-SEA method, the steel panel is divided into square periodic unit cells with length 0.125 m. The finite element model of the periodic unit cell consists of 15 divisions in both directions. 8-nodes shell elements are used for the free wave propagation analysis. In order to determine the direct field response with sufficient accuracy, the acoustic mesh has to be finer for standing waves with higher natural frequencies. The spatial gridspacing is therefore gradually reduced from 3.1 to 1.6 mm for increasing natural frequencies. Contrarily, the wavenumber domain should be meshed finer at lower frequencies to capture the peak of the Green's function and the gridspacing ranges from 0.1 to 1 rad/m over the frequency range of interest.

Figure 3 (a) shows the narrow-band (1/48 octave bands) predictions of the modal peFE-SEA approach and different alternative prediction tools, such as the TMM with a simplified spatial windowing technique (FTMM) [23] and the hybrid mTMM-SEA approach with and without cross modal coupling [11]. The FTMM only takes diffraction effects into account, while the other approaches also include modal behaviour. Clearly, the modal behaviour of the steel panel affects the sound transmission loss up to about 500 Hz as the FTMM prediction coincides with the other methods from that frequency onwards. When comparing the modal peFE-SEA approach with the mTMM-SEA method, a good agreement is found when cross modal coupling is neglected in the mTMM-SEA method as well. The shift (less than 1 dB) between both methods is due to the acoustic mesh refinement in both methods and adopting a finer acoustic mesh would reduce the discrepancy. Comparison with the mTMM-SEA, that accounts for cross modal coupling, shows that the peaks at anti-resonances in the peFE-SEA predictions do not occur, while the dips in the predicted sound transmission loss appear at the same frequencies [11]. Figure 3 (b) compares the predictions with experimental data for which at lower frequencies the modal behaviour of the rooms result in oscillations in the sound transmission loss. Above 250 Hz the diffuse field assumption in the SEA subsystems is justified and there is an overall good agreement.

4 CONCLUSIONS

In this work, a hybridization between two-dimensional periodic finite element modelling and statistical energy analysis has been investigated for simply supported structures. In order to decompose the displacements of the structure into standing waves, the dynamic properties of the unit cell only need to be computed for a specific number of imposed propagation constants. The resulting travelling waves are combined next into standing waves to compute the direct field response, taking special care for zero displacements at the boundaries of the global structure. As a validation example, the sound insulation predictions of a steel plate are compared with other prediction tools and experimental data. The predicted sound transmission loss of the steel plate are in close agreement with the measured sound insulation.

ACKNOWLEDGEMENTS

This research was supported by a PhD Fellowship (C. Decraene) from the Research Foundation - Flanders. The financial support of FWO is gratefuly acknowledged. The first author also thanks Prof. Brian Mace for their discussions at the University of Auckland during her research stay, funded by a travel grant of the FWO.

REFERENCES

[1] Shorter, P.J.; Langley, R.S. Vibro-acoustic analysis of complex systems. Journal of Sound and Vibration, Vol 288 (3), 2005, pp 669-699.

[2] Langley, R.S.; Cotoni, V. Response variance prediction for uncertain vibro-acoustic systems using a hybrid deterministic-statistical method. Journal of the Acoustical Society of America, Vol 122 (6), 2007, pp 3445-3463.

[3] Reynders, E.; Langley, R.S.; Dijckmans, A.; Vermeir, G. A hybrid finite element - statistical energy analysis approach to robust sound transmission modelling. Journal of Sound and Vibration, Vol 333 (19), 2014, pp 4621-4636.

[4] Shorter, P.J.; Langley, R.S. On the reciprocity relationship between direct field radiation and diffuse reverberant loading. Journal of the Acoustical Society of America, Vol 117 (1), 2005, pp 85-95.

[5] Langley, R.S. On the diffuse field reciprocity relationship and vibrational energy variance in a random subsystem at high frequencies. Journal of the Acoustical Society of America, Vol 121 (2), 2007, pp 913-921.

[6] Lauriks, W.; Mees, P.; Allard, J. F. The acoustic transmission through layered systems. Journal of Sound and Vibration, Vol 155 (1), 1992, pp 125-132.

[7] Brouard, B.; Lafarge, D.; Allard, J. F. A general method of modelling sound propagation in layered media. Journal of Sound and Vibration, Vol 183 (1), 1995, pp 129-142.

[8] Allard, J. F.; Atalla, N. Propagation of sound in porous media. John Wiley & Sons, Chichester (UK), 2009.

[9] Dijckmans, A.; Vermeir, G. Development of a hybrid wave based - transfer matrix model for sound transmission analysis. Journal of the Acoustical Society of America, Vol 133 (4), 2013, pp 2157-2168.

[10] Rhazi, D.; Atalla, N. Acoustic and vibration response of a structure with added noise control treatment under various excitations. Journal of the Acoustical Society of America, Vol 135 (2), 2014, pp 693-704.

[11] Decraene, C.; Dijckmans, A.; Reynders, E. Fast mean and variance computation of the diffuse sound transmission through finite-sized thick and layered wall and floor systems. Journal of Sound and Vibration, Vol 422, 2018, pp 131-145.

[12] Cotoni, V.; Langley, R. S.; Shorter, P. J. A statistical energy analysis subsystem formulation using finite element and periodic structure theory. Journal of Sound and Vibration, Vol 318 (4-5), 2008, pp 1077-1108.

[13] Reynders, E.; van hoorickx, C.; Dijckmans, A. Sound transmission through finite rib-stiffened and orthotropic plates. Acta Acustica united with Acustica, Vol 102 (6), 2016, pp 999-1010.

[14] Langley, R.S.; Cordioli, J.A. Hybrid deterministic-statistic analysis of vibro-acoustic systems with domain couplings on statistical components. Journal of Sound and Vibration, Vol 321 (3-5), 2009, pp 893-912.

[15] Cremer, L.; Heckl, M. Structure-borne sound: Structural vibrations and sound radiation at audio frequencies. Springer, Berlin (Germany), 2nd edition, 1988.

[16] Brillouin, L. Wave propagation in periodic structures. Dover Publications, NY (USA), 2nd edition, 1953.

[17] Mead, D.J. A general theory of harmonic wave propagation in linear periodic systems with multiple coupling. Journal of Sound and Vibration, Vol 27 (2), 1973, pp 235-260.

[18] Mead, D.J.; Parthan, S. Free wave propagation in two-dimensional periodic plates Journal of Sound and Vibration, Vol 64 (3), 1979, pp 325-348.

[19] Mead, D.J. Wave propagation in continuous periodic structures: Research contributions from Southampton. Journal of Sound and Vibration, Vol 190 (3), 1996, pp 495-524.

[20] Langley, R.S. A note on the force boundary conditions for two-dimensional periodic structures with corner freedoms. Journal of Sound and Vibration, Vol 167 (2), 1993, pp 377-381.

[21] Williams, E.G.; Maynard, G.D. Numerical evaluation of the Rayleigh integral for planar radiators using the FFT. Journal of Sound and Vibration, Vol 172 (4), 1994, pp 491-511.

[22] Langley, R.S. On the modal density and energy flow characteristics of periodic structures. Journal of the Acoustical Society of America, Vol 72 (6), 1982, pp 2020-2030.

[23] Vigran, T.E. Predicting the sound reduction index of finite size specimen by a simplified spatial windowing technique. Journal of Sound and Vibration, Vol 325 (3), 2009, pp 507-512.